Food Hydrocolloids

Modulating elasticity of heat-set soy protein-curdlan gels by small phenolic acids

--Manuscript Draft--

Manuscript Number:	FOODHYD-D-23-03744R1
Article Type:	Research paper
Keywords:	Plant-based; alternative protein; fish analogue; phase heterogeneity; ferulic acid; trehalose
Corresponding Author:	Pui Yeu Phoon Singapore Institute of Food and Biotechnology Innovation SINGAPORE
First Author:	Pui Yeu Phoon
Order of Authors:	Pui Yeu Phoon
	Amanda Xin Yi Sng
	Nikolai Yakovlev
	Su Hui Lim
	Choy Eng Nge
	Gomathy Sandhya Subramanian
	Sergey Gorelik
	Yoganathan Kanagasundaram
	Maxim Kiryukhin
Abstract:	Fish-gel products with a bouncy texture are integral to the gastronomy of many regions in Asia. Despite the current alternative protein food megatrend driven by sustainability, plant-based fish-gel analogues are not popularised due to the lack of accessible technical know-how in tailoring textural nuances convincingly. Here, we studied how two readily available small phenolic acids, i.e., gallic acid and ferulic acid, had differing interactions with curdlan and soy protein. Noteworthily, we found that when ferulic acid and trehalose were coexistent in mM concentrations at pH 6, (i) permanent interaction between soy protein and ferulic acid at ≥ 40 degree Celsius was mild (as according to precision ellipsometry); (ii) protein aggregation in a bicontinuous microstructure with curdlan network (3% w/w) and auxiliary protein phase (16.2% w/w) was restrained (as according to epifluorescence microscopy); and (iii) comparable to real commercial fishball, the resultant heat-set gel displayed large change in gel stiffness at 60-70% compressive strain; as well as (iv) similar rate in stress-relaxation. We thereby propose a new hydrocolloidal gel design concept: micro-phase heterogeneity and in turn bulk elasticity are influenced by the aggregation conditions of the auxiliary protein phase, as modulatable by phenolic acids. This mechanism opens new possibilities for fine-tuning elastic texture in support of alternative protein innovation in food processing.
Suggested Reviewers:	Kigen Takahashi kigen@kaiyodai.ac.jp
	Jianrong Li lijr6491@163.com
	Manat Chaijan cmanat@wu.ac.th
	Byung-Soo Chun bschun@pknu.ac.kr

Highlights

- Thermo precision ellipsometry probed protein-phenolic acid binding in real-time
- Ferulic and gallic acids were found to affect soy protein aggregation differently
- In a curdlan-soy protein binary system, ferulic acid curbed protein aggregation
- This promoted interweaving of curdlan; micro-phase heterogeneity ensued
- This led to plant-based proteinaceous gel with Asian-style fishball-like bounciness

Graphical Abstract

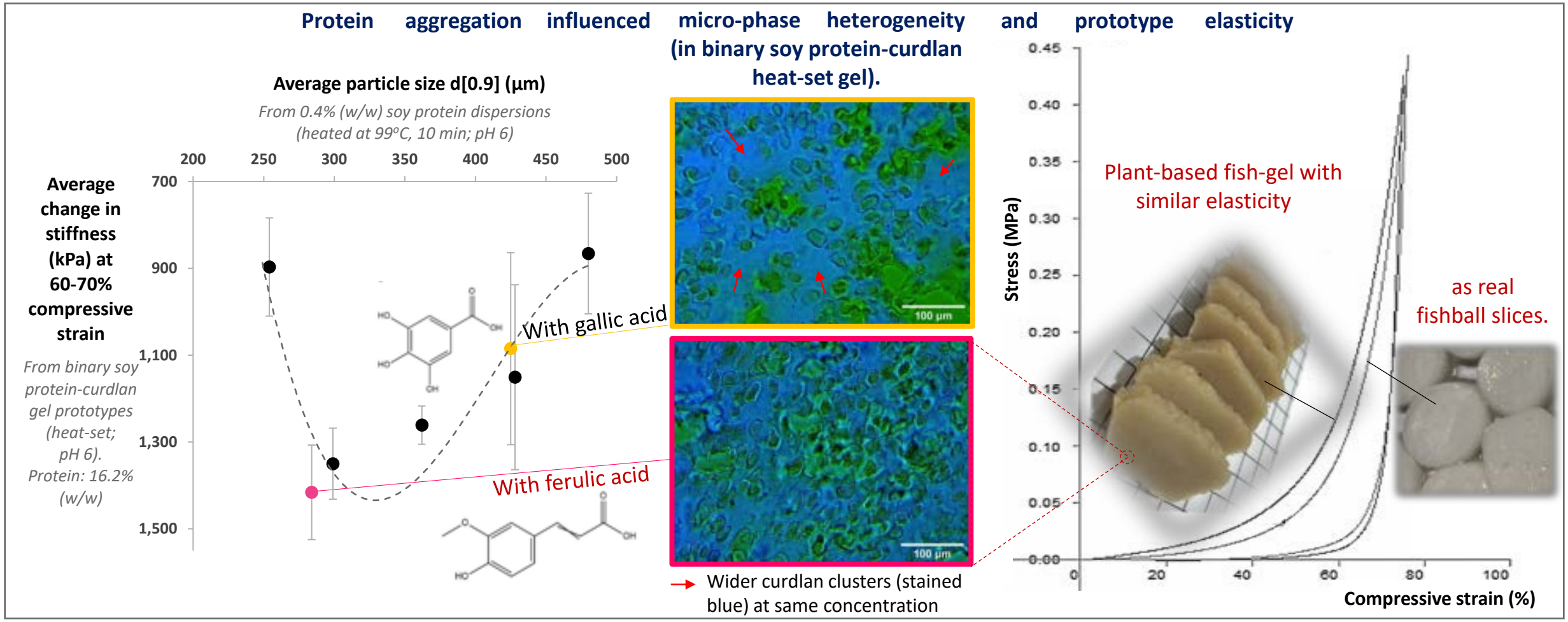

Title

Modulating elasticity of heat-set soy protein-curdlan gels by small phenolic acids

Author names and affiliations

Pui Yeu Phoon,[a]* Amanda Xin Yi Sng,[a] Nikolai Yakovlev,[b] Su Hui Lim,[a] Choy Eng Nge,[a] Gomathy Sandhya Subramanian,[a] Sergey Gorelik,[a] Yoganathan Kanagasundaram,[a] Maxim Kiryukhin.[a1]

[a]Singapore Institute of Food and Biotechnology Technology (SIFBI), Agency for Science, Technology and Research (A*STAR), 31 Biopolis Way, Singapore 138669, Singapore.

[b]Department of Physics, National University of Singapore, Science Drive 4. Singapore 119077, Singapore.

[1]Present address: Life Improvement by Future Technologies (LIFT) Center, 143025, Moscow, Russia.

Email addresses: phoon_pui_yeu@sifbi.a-star.edu.sg; sngxy@sifbi.a-star.edu.sg; phyny@nus.edu.sg; lim_su_hui@sifbi.a-star.edu.sg; ngece@sifbi.a-star.edu.sg; sandhya_subramanian@sifbi.a-star.edu.sg; sergey_gorelik@sifbi.a-star.edu.sg; yoganathank@sifbi.a-star.edu.sg; maximkir@msn.com

*Corresponding author.

1. Introduction

Fish-gel products with a bouncy texture are low-price cultural foods ubiquitous throughout East and Southeast Asia. To formulate convincing non-animal mimetics, besides delivering equivalent protein content (typically 8-10% w/w) if not higher, the main challenge lies in creating a cohesive heat-set gel that exhibits the signature bounciness akin to a rubber ball, featuring non-linear (increasing) change in stiffness during large compressive deformation and low hysteresis during unloading In the current commercial scene of meat and seafood alternatives, transferable and low-cost solutions to Asian-style fish-gel products are limited. For instance, for meat-like burger patty, there is no requirement for elastic/springy texture. Thus, it does not matter that the thermal gelling binders used, from the conventional but synthetic methylcellulose and modified starch to natural agar as used in newer development (Watson, 2020), all form brittle hydrogels. In another instance, while fungi-based precision fermentation holds promise in developing biomasses toward authentic textures and further restructuring, it is presently cost-prohibitive. This is due to hurdles stemming from microbial strain-specific production requirements, feedstock pretreatment, and scaling up production (Southey, 2022).

A plausible direction for formulating realistic Asian-style fish-gel mimetics lies in more purposeful structuring of heat-set gels comprising plant-based protein and carbohydrate hydrocolloid to enable textural refinement. In the academia research front over the past few years, new knowledge creation on thermal gelation of plant-based protein, from soy, yellow pea, field pea, fava bean, kidney bean, lentil to oat origin (Guldiken et al., 2021; Nieto Nieto et al., 2016; Shevkani et al., 2015; Yan et al., 2020; Yang et al., 2021) is sporadic and slow. In a wider scope, research on hydrocolloid-facilitated thermal gelation of protein in surimi processing continues to be relevant in recent years (Chen et al., 2020; Mi et al., 2021; Yuan et al., 2019), as a testament to the regional popularity of fish-gel products. Often, the reported research approaches for testing plant- or fish-based proteinaceous gels are similar, touching on protein secondary structure, water-holding capacity, gel network microstructure, and/or gel strength. The knowledge base is expanded by varying the dosage and type of carbohydrate polymer incorporated. However, the establishment of any causal relation between configuration and texture is weak, or at most one-dimensional with the focus on gel strength. The situation with plant-based protein is at times exacerbated by protein aggregation and loss of techno-functionality during the extraction process, which is not uncommon in commercial plant-based protein isolates/concentrates. The current knowledge base is inadequate in supporting skilful accentuation or toning down of specific textural attributes for industrial product development.

In response, this study investigates the potential of different small phenolic acids to modulate inter-/supra-molecular associations and spatial configuration in a binary polymer system, toward creating

the characteristic bounciness of Asian-style fish-gel in a plant-based protein-based intermediate product. The binary system comprised of thermo-irreversible curdlan gum, a linear β-1,3-glucan in single and triple helical structures that form an elastic network, and a commercial soy protein isolate that was pre-screened for intrinsic gelling strength. Small phenolic acids were chosen for their low molecular weight to reduce the possibility of excessive complexation with protein causing decreased bioavailability (Cirkovic Velickovic & Stanic-Vucinic, 2018). The tested small phenolic acids were (i) gallic acid (molecular weight: 170.12 g/mol, water-soluble with three phenolic hydroxyl groups); and (ii) ferulic acid (molecular weight: 194.18 g/mol, natively poorly water-insoluble, with one methoxyl group and one phenolic hydroxyl group). The poor water-solubility of ferulic acid was counteracted by adding trehalose (Phoon et al., 2022) and increasing the pH to above the pKa of its carboxylic group. Through selected analytical techniques such as food texturometry, solid-state NMR spectroscopy, dynamic mechanical analysis, thermal precision ellipsometry, static light scattering for particle analysis, Raman spectral imaging, and epi-fluorescence microscopy, this paper elucidates how the two small phenolic acids modulate texture differently. This paper also reports the finding of a transformative solution in developing texturally promising product prototypes with >16% protein content, higher than existing commercial benchmarks.

2. Materials and methods

2.1 Materials

Food-grade materials sourced for prototype preparation were as follows: 97.5% pure gallic acid and 99% pure ferulic acid (Penta Manufacturing Company, Livingston, New Jersey, U.S.); curdlan gum (Natural Colloids Industries Pte. Ltd., Singapore); soy protein isolate (SPI) FUJIPRO FR (Fuji Oil Co., Ltd., Osaka, Japan); trehalose in mixed anhydrous and dihydrate forms (Phoon Huat, Singapore). Distilled water was used in all sample preparation. 32% (w/w) hydrochloric acid (HCl) (Sigma-Aldrich, St. Louis, Missouri, U.S.) and sodium hydroxide (NaOH) (Fisher Scientific, Pittsburg, Pennsylvania, U.S.), both food-grade, were the only chemicals used for pH adjustment in samples. Additionally, commercial BoBo brand fishball [ingredients: surimi (fish meat, sugar, egg white powder, sodium triphosphate), salt, monosodium glutamate; protein content from Dumus analysis (average): 10.1% w/w] (Ha Li Fa Pte. Ltd., Singapore) and vegetarian mushroom ball [ingredients: konjac, starch, soy powder, seasoning, chilli, mushroom, vegetable; protein content from label: 13.3% w/w] (Vegetalk Food Supplies Pte Ltd., Singapore), were purchased as references. Homemade fishball reference was also made from supermarket groceries [ingredients: yellowtail fish meat, tapioca flour, salt; protein content from Dumus analysis (average): 14.2 w/w]. Rice bran extract was prepared according to our

recent work (Phoon et al., 2022). Fast Green FCF and sodium 8-anilino-1-naphthalenesulfonate (ANS-Na) staining dyes were obtained from Tokyo Chemical Industry Co., Ltd. (Tokyo Japan).

2.2 Preparation of prototypes and references

Every 70 g of plant-based "fish" paste was made by mixing in a 250 mL beaker using a single strip beater attached to a hand blender (Philips, Amsterdam, Netherlands), at the lowest speed setting for 3 min. As default, SPI (12.6 g) was mixed into a 40-50 ^{o}C pH 6 solution (43.4 g) for 1.5 min, after which curdlan paste (2.1 g curdlan + 11.9 g pH 6 water) was added in for another 1.5 min of mixing. Hence, the protein, curdlan, and water content in each prototype was ≥ 16.2% (assuming minimal 90% protein purity), 3%, and 79% (w/w), respectively. Variations of the pH 6 solution were (i) water $\pm$ trehalose (2.0 mM); (ii) gallic acid (1.0 mM) $\pm$ trehalose (2.0 mM), and (iii) ferulic acid (0.2, 0.5, 1.0, 2.0 mM) $\pm$ trehalose (0.4, 1.0, 2.0, 4.0 mM). Further tested variations included preheating the phenolic acid solutions at 65 ^{o}C for 1 h, mixing the "fish" paste ingredients all at one go for 3 min, and mixing at room temperature (RT). The "fish" paste was transferred to a non-stick rectangular mould (9.9 × 4.6 × 1.5 cm), covered with aluminum foil, and steamed for 15 min.

To create homemade fishball, fish paste was formed from mincing yellowtail fish meat (75.71% w/w), water (20.34% w/w), tapioca flour (2.26% w/w), and salt (1.69% w/w) on a chopping board with the back of a chopper knife. It was shaped and cooked the same way as above. To cook the commercial references, they were cut by a 10-wire luncheon meat slicer into <1.0 cm slices, laid on a tray, also covered with aluminum foil and steamed for 15 min. All steamed samples and references were cooled and stored at 4 ^{o}C.

2.3 Stress strain and stress relaxation analyses

Refrigerated steamed samples were brought to RT the next day, wiped off surface condensate, cut into cylindrical discs of 7.0-8.5 mm height and 13-14 mm diameter, and subjected to uniaxial compression by a SMS P/75 flat, cylindrical compression probe on a TA.XT.plus Texture Analyser (Stable Micro Systems, U.K.), controlled via the Exponent software (version 6.1.16.0). For stress strain analysis (with four technical replicate measurements taken), the test parameters were: (i) level of target mode: 80% strain; (ii) pre-test, test, and post-test speeds: 1, 1, and 2 mm.s^{-1}; respectively. For stress relaxation analysis (with three technical replicate measurements taken), the test parameters were (i) level of target mode: 40% strain; (ii) holding time: 60 s, (iii) pre-test/test/post-test speeds: 1 mm.s^{-1}. For both analyses, the force of trigger type was 5 g (auto).

2.4 Liquid Chromatography-Mass Spectrometry (LC-MS) analysis of small phenolic acid solutions

Aqueous gallic acid (1.0 mM) solution and ferulic acid (1.0 mM) + trehalose (2.0 mM) solution, both at pH 6 and preheated at 65 °C for 1 h, were run on LC-MS as described in an earlier work (Phoon et al., 2022). This was to determine how the preheating affected the molecular weight of the phenolic acids.

2.5 Solid-state 13C cross polarisation magic angle spinning NMR spectroscopy (CP/MAS 13C-NMR)

Considering the insolubility of curdlan in water, solid state CP/MAS 13C-NMR was used to gain insight on curdlan-phenolic acid interaction. Model samples of 10% (w/w) curdlan in various pH 6 solutions, namely (i) water, (ii) trehalose (2.0 mM) solution, (iii) preheated gallic acid (1.0 mM) solution, and (iv) preheated ferulic acid (1.0 mM) + trehalose (2.0 mM) solution, were first heat-set at 90 °C for 15 min. They were then analysed by CP/MAS NMR spectroscopy on an Avance NEO 400 MHz spectrometer (Bruker, Billerica, Massachusetts, U.S.), with full loading on a 4mm ZrO2 CRAMPS rotor. Operation was at a ^{13}C frequency of 100.64 MHz. Five hundred and twelve scans were accumulated for each spectrum with a recycle delay of 5 s. The chemical shifts were referenced to tetramethylsilane using adamantane as an external standard.

2.6 Dynamic mechanical analysis

To complement Section 2.5, selected, actual steamed prototypes were cut one day after 4 °C storage as in Section 2.3, for probing the effect of phenolic acid (specifically ferulic acid) on glass transition (Tg) and storage modulus (G') changes in the skeletal curdlan via dynamic mechanical analysis (DMA). Analysis was done in compression mode on a Q800 Dynamic Mechanical Analyser (TA Instruments, New Castle, Delaware, U.S.) precooled by liquid nitrogen, on the same day of sample cutting and after 1 additional day (16 h) of frozen storage at -20 °C. During which, each sample was clamped with a preload force of 0.07 N and subjected to an oscillating strain amplitude of 50 μm (within 0.6-0.7% strain) at 1 Hz. Each sample was first equilibrated at 0 °C for 1 min, and then underwent a heating ramp at 2 °C/min to at least 37 °C before evaporative moisture loss caused signal interference.

2.7 Thermal precision ellipsometry

Considering the solubility of some of the proteins in SPI, precision ellipsometry (PREL) was used to gain insight on the nature of protein-phenolic acid binding. This was through tracking the incremental, liquid-phase adsorption of alternating soluble protein and phenolic acid layers on an oxidised silicon substrate. Ellipsometry measures the polarisation of light that is reflected by the sample surface, by measuring the phase shift between the perpendicular and parallel components of the polarisation vector. This phase shift, also called ellipticity, is proportional to the accumulative thickness of the

adsorbed layers. The ellipticity is then converted by a quarter-wave retarder into rotation which, in PREL, is measured at high sensitivity down to microradians using a compact polarisation modulator (Yakovlev et al., 2019). This translates to a sensitivity of 0.1 nm of organic layer thickness on the substrate.

Based on a previously reported setup, in which the substrate was held in a glass cuvette with appropriate fluidic system (Lau et al., 2017), we made modifications to enable PREL measurements in liquid at elevated temperatures. We included a glass jacket around the glass cuvette with the substrate. In the jacket, there was degassed water circulating from a stirred water bath in proximity, controlled at the desired temperature (within 25-65 ^{o}C). Immersed in the bath were also heat exchanger tubings, through which rinsing water and solutions of interest were injected and supplied to the cuvette. Connection tubings between the glass jacket and water bath were covered in insulation foam sleeves. At the start of a run, the cuvette holding a clean substrate was filled with water. In blocks of 200 s, we injected amino-propyl-silane (APS) (5 mM) solution to cover the substrate with an anchor layer, rinsed the cuvette with water, and then injected polystyrene sulfonate (PSS) (10 mM) solution to add a linker layer. This way, the substrate became functionalised. Thereafter, the desired water bath temperature was set. Once it stabilised, the supernatant from an aqueous dispersion of 0.4% hexane-defatted SPI (centrifuged at 1800 ×g for 15 min) and the tested phenolic acid (2.5 mM) solution (i.e., either gallic acid, or ferulic acid with 5.0 mM trehalose), both at pH 6, were injected in alternate successions in 200 s blocks. In between solution injections, there was 200 s of intermediate rinsing with water to remove non-permanently adsorbed molecules. As captured quantitatively by PREL in real time, any increment in recorded thickness which was not reversed by water rinsing would signal permanent molecular binding.

2.8 Particle size analysis

To complement Section 2.7, protein aggregation induced by heating with/without phenolic acid was studied by static light scattering. In 50-mL centrifuge tubes filled to 43.5 g of contents, dispersions of 0.4% hexane-defatted SPI in selected pH 6 solutions from Section 2.2 were heated at 99 ^{o}C for 10 min, cooled in RT water, and stored at 4 ^{o}C. The next day, they were analysed on a Mastersizer 2000 laser diffraction particle size analyser (Malvern Panalytical, Malvern, U.K.). Three technical replicate measurements were taken.

2.9 Microscopy

40-µm thick sections of selected steamed samples, sliced by a Leica CM3050 S cryotome (Leica Biosystems, Wetzlar, Germany), were laid on microscopy slides and imaged according to Sections 2.9.1 and 2.9.2.

2.9.1 Raman spectral imaging

A confocal Raman microscope, Renishaw inVia™ (Renishaw plc., Wotton-under-Edge, U.K.) was used at 532 nm excitation, with 50% laser power, 50× objective (0.5 NA), and 2400 l/mm grating. The beam spot on the sample was ~2 µm. Raman spectra from 50 µm × µm area were recorded point by point using raster scanning. Raman spectra in the spectral range 640 to 1800 cm^{-1} were acquired with 0.2 s exposure time per point. To visualise the spatial distribution of components, baseline-subtracted Raman intensity images were generated for two specific Raman bands: 1000 cm^{-1} (phenyl ring breathing of phenylalanine in SPI) and 1130 cm^{-1} (C-O band for the glucose β-anomer subunit in curdlan). A WiRE 5.2 software (Renishaw plc.) was used for the data analysis.

2.9.2 Epi-flurorescence microscopy

Each section was stained with few drops of 0.01% (w/w) Fast Green FCF for at least 2 min, rinsed gently with Milli-Q® water without being dislodged, stained next with few drops of 1% (w/w) ANS-Na, and similarly rinsed again with Milli-Q®. Epifluorescence microscopy was performed on an Olympus BX53 upright microscope with both DAPI (4',6-diamidino-2-phenylindole) and FITC (fluorescein) bandpass filters. Images were captured by an Olympus microscope digital camera DP74 connected to a cellSans software (Olympus, Tokyo, Japan), and adjusted in brightness and contrast using the image processing software Fiji. These micrographs were also converted to binary images in Fiji using minimal and standardised procedural settings, to quantify the different extent of clustering in the curdlan phase.

2.10 Statistical analysis

Results from Sections 2.3 and 2.8 were analysed using an online calculator for one-way ANOVA with Tukey HSD post-hoc test (Lane, 2017).

3. Results and discussion

3.1 Developing plant-based Asian-style fish-gel mimetics with high protein content and authentic texture

Texture profile analysis, which comprised of two cycles of compression with a brief rest in seconds in between, was done at 60% compressive strain so as not to exceed the point of fracturability as seen in the commercial vegetarian ball (Figure 1A). It yielded springiness values mostly within a narrow range of 0.9-1.0, not being able to capture significant differences among the most sensorially

dissimilar samples as pointed out by some authors (Bourne, 1978; Szczesniak, 1963). Meanwhile, the high content of aggregating plant protein in the samples led to large standard deviation in conventional small-amplitude oscillatory shear measurements. As such, data for both tests were not used. Instead, taking a real fishball as reference, success in mimicking a bouncy texture could be gauged by the comparability in stress-strain profile and hysteresis during high strain (e.g., 60-70%) compression which emulates mastication. Despite similar elastomer (i.e. myofibrillar) network, this change in stiffness was significantly steeper in commercial fishball (1525 kPa) than in homemade fishball (935 kPa) (Figure 1A, Table 1A), evidently an effect of scaling law relation with moisture content (Li et al., 2020): the former had 89.3% (w/w) moisture on average and the latter 82.9 % (w/w) (from oven drying determination). Although the homemade fishball had closer protein and moisture content as the plant-based samples (i.e., protein: 14.2 to ≥ 16.2% w/w; moisture: 79 to 82.9% w/w), the locally popular BoBo commercial fishball would serve as a more reliable and objective benchmark in terms of expectation of bounciness, albeit raising the bar higher for imitation. Nonetheless, successful plant-based prototypes were developed at pH 6 using minimal natural ingredients, comprising only water, plant-based protein isolate, hydrocolloid, and solubilised ferulic acid with trehalose. The close textural resemblance to a cooked real fishball was evidenced by similar change in stiffness up to 60-70% compressive strain (i.e., 1416-1525 kPa) (Figure 1A, Table 1A). The development offers a marked improvement over a typical commercial vegetarian ball which is disproportionately stiff and crunchy, as discernible from faster average rate of stress-relaxation from 40% compression strain (i.e., 0.422) (Figure 1B), too steep stress-stain gradients at <60% strain (Figure 1A), and the surfacing of fracture points in the stress-strain curve at >60% strain (Figure 1A). A minor drawback in the successful ferulic-acid based prototypes was that their higher protein content gave rise to denser structure and thus larger force measurements across 40-70% strain (i.e., greater firmness than cooked commercial fishball) (data not shown).

The success with ferulic acid could not be replicated by rice bran extract (Table 1A), which was found to be a natural source of ferulic acid according to LC-MS analysis from our previous study (Phoon et al., 2022). Thus, the purity of ferulic acid matters. Besides, there was an apparent optimal concentration of ~1 mM ferulic acid in the pH 6 solution for mixing with SPI during prototype making (Table 1B), which translated to 0.012% (w/w) ferulic acid in the cooked prototype (assuming negligible evaporative moisture loss). The optimal dosage underscores the significance of controlled molecular interaction between SPI and phenolic acid. Excessive interaction (with 2 mM ferulic acid in the pH 6 solution) adversely impacted the change in stiffness at 60-70% compressive strain, as noticed in the value drop from 1416 kPa (with 1 mM ferulic acid) to 1306 kPa. Conversely, under conditions which

restricted SPI-ferulic acid intermolecular collisions, e.g., lower temperature mixing (denoted as *RT-mix* in Table 1) and higher mix viscosity arising from all ingredients including curdlan mixed at one go (denoted as *1-mix* in Table 1), the change in stiffness at 60-70% strain was also lower in magnitude (i.e., 1068-1122, 1380 kPa, as opposed to 1416-1420 kPa) (Table 1C). In addition, the co-existence of trehalose mattered, as ferulic acid alone at the optimal concentration led to lower change in stiffness (i.e., 1261-1350 kPa) (Table 1C). The dosage of co-existing trehalose for higher change in stiffness does not need to be high—with 0.012% (w/w) ferulic acid, 0.045% (w/w) trehalose (i.e., 1:2 ferulic acid-trehalose molar ratio) was found to suffice.

3.2 Assessment of oxidation in phenolic acids

An original hypothesis was that if small phenolic acids were oxidised to quinones, the latter could attack nucleophilic amino acids to form adducts (Tang et al., 2017) to further promote cross-linking in protein gelation. Due to low-cost expectation of making plant-based fishball mimics and societal inclination toward natural food processing, the attempt on oxidising ferulic acid and gallic acid was limited to conventional heating in this work. The LC-MS results reveal that by pre-heating the solutions of both phenolic acids at 1 mM concentration at 65 ^{o}C for 1 h (denoted as *prh* in Table 1), the increase in molecular size was only marginal. A peak with accurate mass 264.027, putatively identified as purpurogallin-4-carboxylic acid (digallic acid oxidation product), was detected at ~6% relative to gallic acid based on peak area in the extracted ion chromatograms (EIC) (positive mode) (Figures 2A, C). Two possible di-ferulic acid oxidised product masses of 340.094 and 386.1002 were detected, but their combined presence amounted to <2% relative to ferulic acid based on peak area (Figures 2B, D). The minimal impact of *prh* could explain the lack of significant difference between prototype pairs prepared in the same way except with or without it. The different outcome from the use of ferulic acid versus gallic acid was unlikely to stem from oxidation.

3.3 Interpretation of binding between phenolic acids and curdlan

Figure 3 compares the NMR spectra of curdlan pre-heated with and without the dosage of phenolic acid and trehalose. For the NMR analysis, the phenolic acid dosage was 10 µmol per gram of curdlan, which was close to the actual dosage tested in most of the prototypes (12.8 µmol per gram of curdlan). Thus, any spectral change would representatively suggest that curdlan-phenolic acid molecular interactions in a prototype are non-covalent interactions (hydrogen bonds, hydrophobic interactions, and electrostatic and ionic interactions). Figure 3 depicts peak broadening at C2, C3, and C5 of the glucose monomer of curdlan in the presence of ferulic acid (Figure 3D) as compared to the corresponding control (Figure 3B), suggesting a change in conformations after accounting for

trehalose. Apparent peak broadening at C2 and C5 was also observed in the spectrum with gallic acid (Figure 3C) as compared to its corresponding control (Figure 3A). However, the changes observed with the presence of gallic acid (Figure 3C) were smaller than those observed with ferulic acid (Figure 3D), and also contrary to confirmatory literature report of gallic acid binding non-covalently with other soluble carbohydrate hydrocolloids, e.g., at 133 μmol per gram of oat β-glucan (Tudorache et al., 2020). Our finding here for gallic acid might be owing to the lower gallic acid-hydrocolloid weight ratio.

Due to the inconclusive NMR result for curdlan-ferulic acid interaction, DMA comparison was done on prototypes with and without ferulic acid. Considering the typically low entropy of mixing protein and polysaccharide (Grinberg & Tolstoguzov, 1997), and that the prototype preparation involved high-viscosity short-time mixing, one would not expect yielding a microscopically homogeneous blend characterised by only one glass transition temperature (Zhang et al., 2023) between hydrated protein and hydrated curdlan. The general immiscibility between protein and polysaccharide, which existed in distinctly separate domains at the microscale, was also confirmed by Raman confocal spectral imaging with high axial optical resolution (Figure 4). Figure 5 shows the duplicate graphs of DMA , for prototypes with and without ferulic acid, done in compression mode. Inferring from literature Tg values for soy 7S and 11S globulin fractions with 25-40% (w/w) moisture content (Mizuno et al., 2000; Morales & Kokini, 1997), the Tg of hydrated SPI in our prototypes, which had 79% (w/w) water, should be far below -17 ^{o}C hypothetically. Therefore, in Figure 5, one could associate the drop in normalised G' at ≥15 ^{o}C with the glass transition in hydrated curdlan, with its Tg quantitated from the intersection between extending lines from the starting and middle points of the dipping curve. The overlapping Tg results (within 15.0-17.7 ^{o}C) between the prototypes with and without ferulic acid verified that, curdlan-ferulic acid molecular interaction would not be the reason behind the significantly higher change in stiffness (at 60-70% strain) observed for some of the ferulic acid-containing prototypes. We subjected the prototypes to overnight freeze-concentration with the intention of inducing strong aggregation (Niu & Panyam, 2017) among curdlan helices, to accentuate any difference in the curdlan backbone mobility that might be caused by ferulic acid and expressed in a Tg shift. However, this was found not to be the case (Figure 5B), unlike how 3% (w/w) curdlan gel was rendered more freeze-thaw stable by 5% (w/w) erythritol through hydrogen bond reinforcement (Tao et al., 2021). Incidentally, we also did not find a significantly different Tg in the prototype with gallic acid (data not shown). As matters stand, there was no indicative finding of strong curdlan-phenolic acid interaction to influence the physical functionality of curdlan.

3.4 Interpretation of binding between phenolic acids and soy protein

Interaction between soy protein and phenolic acid was revealed by PREL to be permanent when it was induced by heating at 40 °C and above (Figure 6, Supplementary Figure 1). To observe it, in each PREL sample run, two or three cycles of alternating soluble protein and phenolic acid were done. At room temperature, the relative steep increase in deposited thickness from the first adsorbed protein was due to its lower confirmational flexibility, but there was no consistent growth in thickness with subsequent circulations. At 40 °C and higher temperatures, the first protein layer had lower thickness than at room temperature, but subsequently there was increase in the thickness of material progressively adsorbed for both protein-gallic acid and protein-ferulic acid combinations (data for protein-trehalose circulations as control, while not displayed, did not show increasing thickness). By 50 °C, after three cycles, the certainty in attaining permanent material adsorption of ≥2.2 nm in thickness was lower with ferulic acid than with gallic acid (as visually cued by the ~2.2 nm horizontal demarcation line). This might be due to ferulic acid having only one phenolic hydroxyl group available for hydrogen bonding with protein, compared to three in gallic acid.

Non-covalent interactions between protein and phenolic acid are mainly associated by hydrophobic forces, and subsequently stabilised by hydrogen-bonding (Shahidi & Dissanayaka, 2023). Gallic acid has stronger binding interaction over ferulic acid with protein to form more stable protein-phenolic acid aggregate. This is owing to the larger number of phenolic hydroxyl groups available for hydrogen-bonding with carbonyl groups from protein peptide bonds, to stabilise the aggregate. Whereas, with its weaker binding to protein molecules, ferulic acid apparently restrained protein-protein interactions and in turn protein aggregation (Olsson & Swenson, 2019). As indicated in Table 2, the ability of ferulic acid to curb heat-induced protein aggregation was in general only second to trehalose (e.g., d[0.9]: 299 vs 254 μm). Table 2 also shows the comparable (d[0.9]: 425-480 μm), if not greater promotive effect (d[4,3]: 241-259 vs. 192 μm; d[0.5]: 218-230 vs. 186 μm) of gallic acid on protein aggregation compared to the negative control, which was uninhibited by the co-presence of trehalose.

Presumably, a phytochemical which was shown by PREL not to bind to soluble soy protein at room temperature, and only moderately so at higher temperatures, would produce a more elastic plant-based fishball prototype at high compressive strain. In our extended investigation, we observed the same with black tea and green tea aqueous extracts, whereas with tannic acid—a larger phenolic acid (molecular weight: 1701.2 g/mol) with multiple phenolic hydroxyl groups and shown by PREL to bind to soluble soy protein even at room temperature—its corresponding prototype was less elastic (data not shown). Our approach is novel, compared to relevant prior art which encourages protein-protein crosslinking using a reactive phenolic compound but without deep-diving into the causal effect (Zhou et al., 2022).

3.5 Spatial distribution of components in the matrix: how ferulic acid and gallic acid modulate texture differently

In the epi-fluorescent images of both their corresponding prototype matrices, wider spatial inclusions of curdlan as stained by ANS-Na were observed in the bicontinuous microstructure (Figures 7A-B). In contrast, in a prototype matrix containing ferulic acid and trehalose, curdlan was better interweaved with soy protein to yield a more intricate micro-phase heterogeneity at the mesoscale (below 100 μm) (Figure 7C).

Very recently, new perspectives on the relation between micro-phase heterogeneity and macro-mechanical properties have emerged. Fernández-Rico et al. (2022) theorised that in a composite material, mechanical stresses from an integrant elastic network could suppress the separation of phases, thereby arresting varied spatial distribution of the dispersed phase in terms of drop size, number, and shape (Fernández-Rico et al., 2022). The quenching could originate, for instance, from strain-stiffening polymers (Kothari & Cohen, 2020) or the application of heat or pressure. Reversely, as proposed by Maciel et al. (2023), the configurational density of the dispersed phase at the mesoscale could tailor the bulk storage modulus of composite gels, regardless of its state of matter. This could be in the manner of varied packing density in crosslinked species or nanoaggregate clusters, juxtaposed with a separated viscous phase (Maciel et al., 2023). Other reported examples of micro-phase heterogeneity, from gastric mucus (Bansil et al., 2013), concentrated suspension of nearly hard spheres (Pusey & van Megen, 1986), to concentrated emulsion gel with interacting but non-coalesced oil droplets (Tan & Phoon, 2023), corroborated the positive correlation between microstructural heterogeneity and bulk strength. In this study, the prototypes appear to instantiate the causal effect of micro-phase heterogeneity specifically on bulk compressive elasticity at high strain levels that emulate mastication. For which, we propose a new concept whereby the spatial distribution of curdlan, which provides the primary elastic support, is influenced by the aggregation conditions of soy protein as modulated by phenolic acids. We postulate that in prototype preparation, during mixing of the same concentrations of polymers, the proteinaceous aggregate sizes influenced the penetration of curdlan through the matrix, thereby determining the sizes of curdlan inclusions. As Maciel et al. (2023) raised, there might be an optimal basic unit size for micro-phase heterogeneity. While the gallic-acid dosed prototypes and negative control had larger protein aggregates and the positive control had the smallest, they all displayed weaker elasticity at 60-70% compressive strain levels compared to cooked commercial fishball. In contrast, selective prototypes dosed with ferulic acid and trehalose combined had moderate-sized protein aggregates and statistically comparable elasticity as the real fishball. The intricate curdlan network in such a ferulic acid-and-trehalose-based prototype

(Figure 6C) shares a commonality with the elastic colloidal gel model according to the Cauchy-Born theory (Whitaker et al., 2019), in that elasticity emerges mainly from high interconnectedness across local clusters.

4. Conclusions

In this study, we developed binary protein-hydrocolloid gel matrices with curdlan providing skeletal elastic support, as plant-based mimetics of Asian-style fish-gel products with high protein content (at least 16.2% w/w). We showed that with the same concentrations of food polymers, micro-phase heterogeneity could influence bulk compressive elasticity under 60-70% strain, depending on aggregation sizes in the auxiliary proteinaceous phase as modulated by small phenolic acids. Particularly, using soy protein isolate as model protein, we found that a very low dosage of solubilised ferulic acid (0.012% w/w) with co-existing trehalose (0.045% w/w) sufficed to control protein aggregation sizes, for the interweaving of both curdlan and protein phases to create the signature bouncy texture. This new material design concept that we introduce bears implication for the quality of the protein ingredient, which should have adequate water-solubility besides intrinsic gelling strength. We see the potential of this technical concept to explore wider texturising potential in hydrocolloid-phytochemical-plant-based protein matrices, to cater to other unique contexts of food processing and application.

Declarations of interest

None.

Author contributions

Pui Yeu Phoon: Conceptualisation, Formal analysis, Funding acquisition, Investigation, Methodology, Validation, Visualisation, Writing - original draft, Writing - review & editing. **Amanda Xin Yi Sng**: Formal analysis, Investigation, Methodology, Validation, Visualisation, Writing - review & editing. **Nikolai Yakovlev**: Formal analysis, Investigation, Methodology, Validation, Visualisation, Writing - review & editing. **Lim Su Hui**: Formal analysis, Investigation, Methodology, Validation, Visualisation, Writing - review & editing. **Nge Choy Eng**: Formal analysis, Methodology, Validation, Writing - review & editing. **Gomathy Sandhya Subramanian**: Formal analysis, Investigation, Methodology, Validation, Visualisation, Writing - review & editing. **Sergey Gorelik**: Methodology, Validation, Writing - review & editing. **Yoganathan Kanagasundaram**: Validation, Writing - review & editing. **Maxim Kiryukhin**: Validation, Writing - review & editing.

Funding

This work was supported by the 2021 SIFBI Seed Grant [project number SSG21-08]. The funding source is not involved in the study design; in the collection, analysis, and interpretation of data; in the writing of the report; and in the decision to submit the article for publication.

References

Bansil, R., Celli, J., Hardcastle, J., & Turner, B. (2013). The influence of mucus microstructure and rheology in Helicobacter pylori infection. *Frontiers in immunology*, *4*, 310. https://doi.org/10.3389/fimmu.2013.00310

Bourne, M. C. (1978). Texture profile analysis. *Food Technology*, *32*, 62-66.

Chen, J., Deng, T., Wang, C., Mi, H., Yi, S., Li, X., & Li, J. (2020). Effect of hydrocolloids on gel properties and protein secondary structure of silver carp surimi. *Journal of the Science of Food and Agriculture*, *100*(5), 2252-2260. https://doi.org/10.1002/jsfa.10254

Cirkovic Velickovic, T. D., & Stanic-Vucinic, D. J. (2018). The role of dietary phenolic compounds in protein digestion and processing technologies to improve their antinutritive properties. *Comprehensive Reviews in Food Science and Food Safety*, *17*(1), 82-103. https://doi.org/10.1111/1541-4337.12320

Fernández-Rico, C., Sai, T., Sicher, A., Style, R. W., & Dufresne, E. R. (2022). Putting the squeeze on phase separation. *JACS Au*, *2*(1), 66-73. https://doi.org/10.1021/jacsau.1c00443

Grinberg, V. Y., & Tolstoguzov, V. B. (1997). Thermodynamic incompatibility of proteins and polysaccharides in solutions. *Food Hydrocolloids*, *11*(2), 145-158. https://doi.org/10.1016/S0268-005X(97)80022-7

Guldiken, B., Stobbs, J., & Nickerson, M. (2021). Heat induced gelation of pulse protein networks. *Food Chemistry*, *350*, 129158. https://doi.org/10.1016/j.foodchem.2021.129158

Kothari, M., & Cohen, T. (2020). Effect of elasticity on phase separation in heterogeneous systems. *Journal of the Mechanics and Physics of Solids*, *145*, 104153. https://doi.org/10.1016/j.jmps.2020.104153

Lane, D. (2017). *Analysis of variance from summary data*. https://statpages.info/anova1sm.html

Lau, H. H., Murney, R., Yakovlev, N. L., Novoselova, M. V., Lim, S. H., Roy, N., Singh, H., Sukhorukov, G. B., Haigh, B., & Kiryukhin, M. V. (2017). Protein-tannic acid multilayer films: A multifunctional material for microencapsulation of food-derived bioactives. *Journal of Colloid and Interface Science*, *505*, 332-340. https://doi.org/10.1016/j.jcis.2017.06.001

Li, Z., Liu, Z., Ng, T. Y., & Sharma, P. (2020). The effect of water content on the elastic modulus and fracture energy of hydrogel. *Extreme Mechanics Letters*, *35*, 100617. https://doi.org/https://doi.org/10.1016/j.eml.2019.100617

Maciel, B. R., Wang, K., Müller, M., Oelschlaeger, C., & Willenbacher, N. (2023). Targeted micro-phase separation – A generic design concept to control the elasticity of extrudable hydrogels. *Materials & Design*, *227*, 111803. https://doi.org/10.1016/j.matdes.2023.111803

Mi, H., Li, Y., Wang, C., Yi, S., Li, X., & Li, J. (2021). The interaction of starch-gums and their effect on gel properties and protein conformation of silver carp surimi. *Food Hydrocolloids*, *112*, 106290. https://doi.org/10.1016/j.foodhyd.2020.106290

Mizuno, A., Mitsuiki, M., & Motoki, M. (2000). Effect of transglutaminase treatment on the glass transition of soy protein. *Journal of Agricultural and Food Chemistry*, *48*(8), 3286-3291. https://doi.org/10.1021/jf9911500

Morales, A., & Kokini, J. L. (1997). Glass transition of soy globulins using differential scanning calorimetry and mechanical spectrometry. *Biotechnology Progress*, *13*, 624-629. https://doi.org/10.1021/bp9700519

Nieto Nieto, T. V., Wang, Y., Ozimek, L., & Chen, L. (2016). Improved thermal gelation of oat protein with the formation of controlled phase-separated networks using dextrin and carrageenan

polysaccharides. *Food Research International*, *82*, 95-103. https://doi.org/10.1016/j.foodres.2016.01.027

Niu, L., & Panyam, J. (2017). Freeze concentration-induced PLGA and polystyrene nanoparticle aggregation: Imaging and rational design of lyoprotection. *Journal of Controlled Release*, *248*, 125-132. https://doi.org/10.1016/j.jconrel.2017.01.019

Olsson, C., & Swenson, J. (2019). The role of disaccharides for protein–protein interactions – a SANS study. *Molecular Physics*, *117*, 1-9. https://doi.org/10.1080/00268976.2019.1640400

Phoon, P. Y., Sng, A. X. Y., Nge, C. E., & Henry, C. J. (2022). Solubilised rice bran ferulic acid has potential to retard cooked rice retrogradation and not impact digestibility. *Journal of Functional Foods*, *99*, 105330. https://doi.org/10.1016/j.jff.2022.105330

Pusey, P. N., & van Megen, W. (1986). Phase behaviour of concentrated suspensions of nearly hard colloidal spheres. *Nature*, *320*(6060), 340-342. https://doi.org/10.1038/320340a0

Shahidi, F., & Dissanayaka, C. S. (2023). Phenolic-protein interactions: insight from in-silico analyses – a review. *Food Production, Processing and Nutrition*, *5*, Article 2. https://doi.org/10.1186/s43014-022-00121-0

Shevkani, K., Singh, N., Kaur, A., & Rana, J. C. (2015). Structural and functional characterization of kidney bean and field pea protein isolates: A comparative study. *Food Hydrocolloids*, *43*, 679-689. https://doi.org/10.1016/j.foodhyd.2014.07.024

Southey, F. (2022). *Experts outline 'biggest obstacles' facing precision fermentation sector: 'We have brilliant people with brilliant innovations, but can this make money?'*. FoodNavigator Europe. Retrieved 31 July 2023 from https://www.foodnavigator.com/Article/2022/04/19/Experts-outline-biggest-obstacles-facing-precision-fermentation-sector-We-have-brilliant-people-with-brilliant-innovations-but-can-this-make-money

Szczesniak, A. S. (1963). Classification of Textural Characteristics. *Journal of Food Science*, *28*, 385-389.

Tan, Z. L. A., & Phoon, P. Y. (2023). Developing concentrated emulsion gel hybrids structured by natural food fibres. *Food Hydrocolloids*, *145*, 109037. https://doi.org/10.1016/j.foodhyd.2023.109037

Tang, C.-b., Zhang, W.-g., Zou, Y.-f., Xing, L.-j., Zheng, H.-b., Xu, X.-l., & Zhou, G.-h. (2017). Influence of RosA-protein adducts formation on myofibrillar protein gelation properties under oxidative stress. *Food Hydrocolloids*, *67*, 197-205. https://doi.org/10.1016/j.foodhyd.2017.01.006

Tao, H., Wang, B., Wen, H., Cui, B., Zhang, Z., Kong, X., & Wang, Y. (2021). Improvement of the textural characteristics of curdlan gel by the formation of hydrogen bonds with erythritol. *Food Hydrocolloids*, *117*, 106648. https://doi.org/10.1016/j.foodhyd.2021.106648

Tudorache, M., McDonald, J.-L., & Bordenave, N. (2020). Gallic acid reduces the viscosity and water binding capacity of soluble dietary fibers. *Food & Function*, *11*, 5866-5874. https://doi.org/10.1039/D0FO01200A

Watson, E. (2020). *Citrus fiber can help plant-based dairy and meat brands clean up labels, says Fiberstar*. FoodNavigator USA. Retrieved 1 October 2021 from https://www.foodnavigator-usa.com/Article/2020/01/27/Citrus-fiber-can-help-plant-based-dairy-and-meat-brands-clean-up-labels-says-Fiberstar

Whitaker, K. A., Varga, Z., Hsiao, L. C., Solomon, M. J., Swan, J. W., & Furst, E. M. (2019). Colloidal gel elasticity arises from the packing of locally glassy clusters. *Nature Communications*, *10*(1), 2237. https://doi.org/10.1038/s41467-019-10039-w

Yakovlev, N. L., Quek, H. C., Dąbrowski, K. M., & Birch, W. R. (2019). Kinetics of small molecule adsorption studied using precision ellipsometry. *Surface and Interface Analysis*, *51*(7), 697-702. https://doi.org/10.1002/sia.6637

Yan, W., Yin, L., Li, J., & Jia, X. (2020). Development of corn fiber gum–soybean protein isolate double network hydrogels through synergistic gelation. *Food and Bioprocess Technology*, *13*. https://doi.org/10.1007/s11947-020-02412-1

Yang, J., Zamani, S., Liang, L., & Chen, L. (2021). Extraction methods significantly impact pea protein composition, structure and gelling properties. *Food Hydrocolloids*, *117*, 106678. https://doi.org/10.1016/j.foodhyd.2021.106678

Yuan, L., Yu, J., Mu, J., Shi, T., Sun, Q., Jin, W., & Gao, R. (2019). Effects of deacetylation of konjac glucomannan on the physico-chemical properties of surimi gels from silver carp (Hypophthalmichthys molitrix) [10.1039/C9RA03517F]. *RSC Advances*, *9*(34), 19828-19836. https://doi.org/10.1039/C9RA03517F

Zhang, L., Xu, L., Ma, J.-K., Ye, Y.-Y., Chen, Y., & Qian, J.-Y. (2023). Introduction of curdlan optimizes the comprehensive properties of methyl cellulose films. *Foods*, *12*(3), 547. https://doi.org/10.3390/foods12030547

Zhou, Y., Ng, R. X. E., Vijayan, P., Huang, D., & Chen, Y. J. (2022). *Plant based food products and methods of fabrication thereof* (PCT/SG2022/050508). WIPO. https://patentscope.wipo.int/search/en/detail.jsf?docId=WO2023003510&_cid=P20-LSIDM9-43183-1

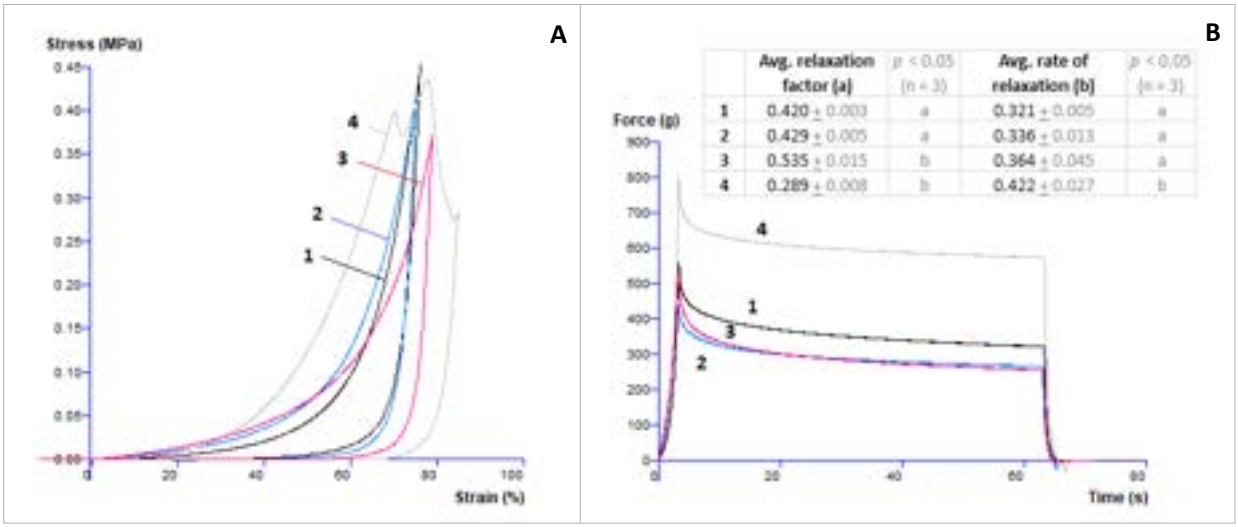

	Avg. relaxation factor (a)	$p < 0.05$ ($n = 3$)	Avg. rate of relaxation (b)	$p < 0.05$ ($n = 3$)
1	0.420 ± 0.003	a	0.321 ± 0.005	a
2	0.429 ± 0.005	a	0.336 ± 0.013	a
3	0.535 ± 0.015	b	0.364 ± 0.045	a
4	0.289 ± 0.008	b	0.422 ± 0.027	b

Figure 1. Representative stress-strain (A) and stress-relaxation (B) curves (from uniaxial compression at room temperature at >70% and 60% strain, respectively) of cooked fishball and its mimics, pre-cut into cylindrical discs of 7.0-8.5 mm height and 13-14 mm diameter. The embedded table shows processed data in terms of (a) average relaxation factor and (b) average dimensionless relaxation rate (± standard deviation) from the stress-relaxation curves, analysed by one-way ANOVA with Tukey HSD post-hoc test. (1) BoBo brand commercial fishball. (2) Successful prototype made from ferulic acid (1.0 mM) + trehalose (2.0 mM) solution, for which the mixing of ingredients during processing involved sequential addition of ingredients at 40-50 °C. (3) Homemade fishball. (4) Commercial vegetarian mushroom ball.

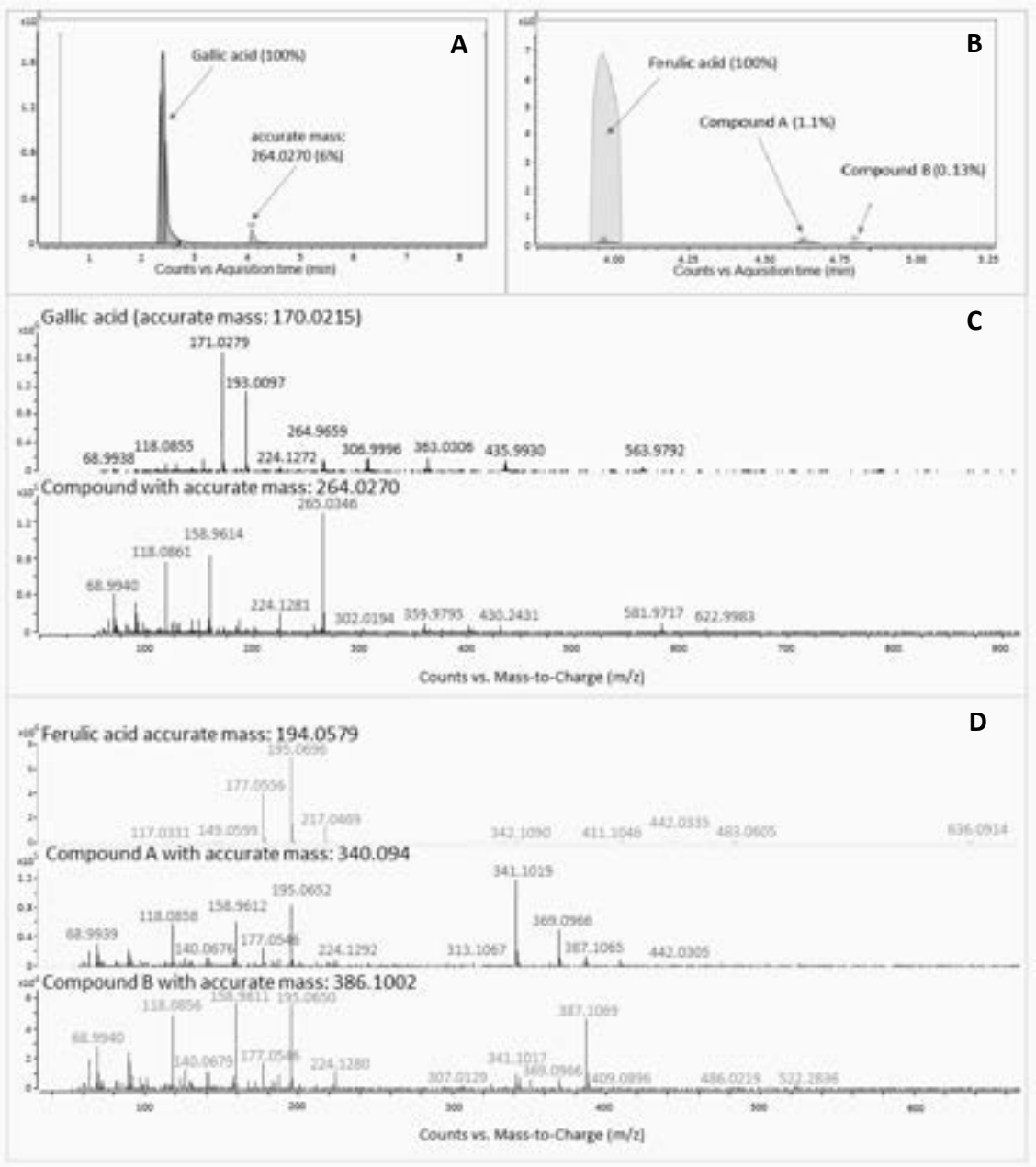

Figure 2. Liquid chromatography and mass spectrometry analyses (positive mode) of pH 6 solutions of (A, C) gallic acid and (B, D) ferulic acid at 1.0 mM, both preheated at 65 °C for 1 h.

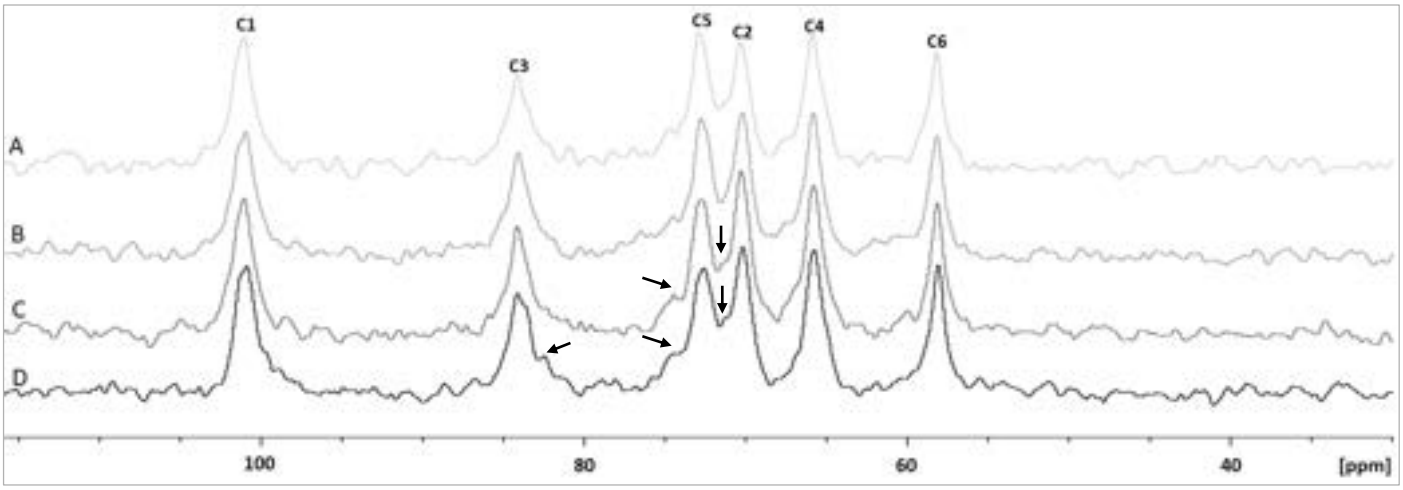

Figure 3. Solid state CP/MAS ^{13}C-NMR spectra of model 10% (w/w) curdlan gels heat-set in various pH 6 solutions. (A) Water. (B) Trehalose (2.0 mM) solution. (C) Gallic acid (1.0 mM) solution that was preheated at 65 °C for 1 h. (D) Ferulic acid (1.0 mM) + trehalose (2.0 mM) solution that was preheated at 65 °C for 1h. Heat-setting conditions: 90 °C, 15 min. Black arrows indicate peak broadening.

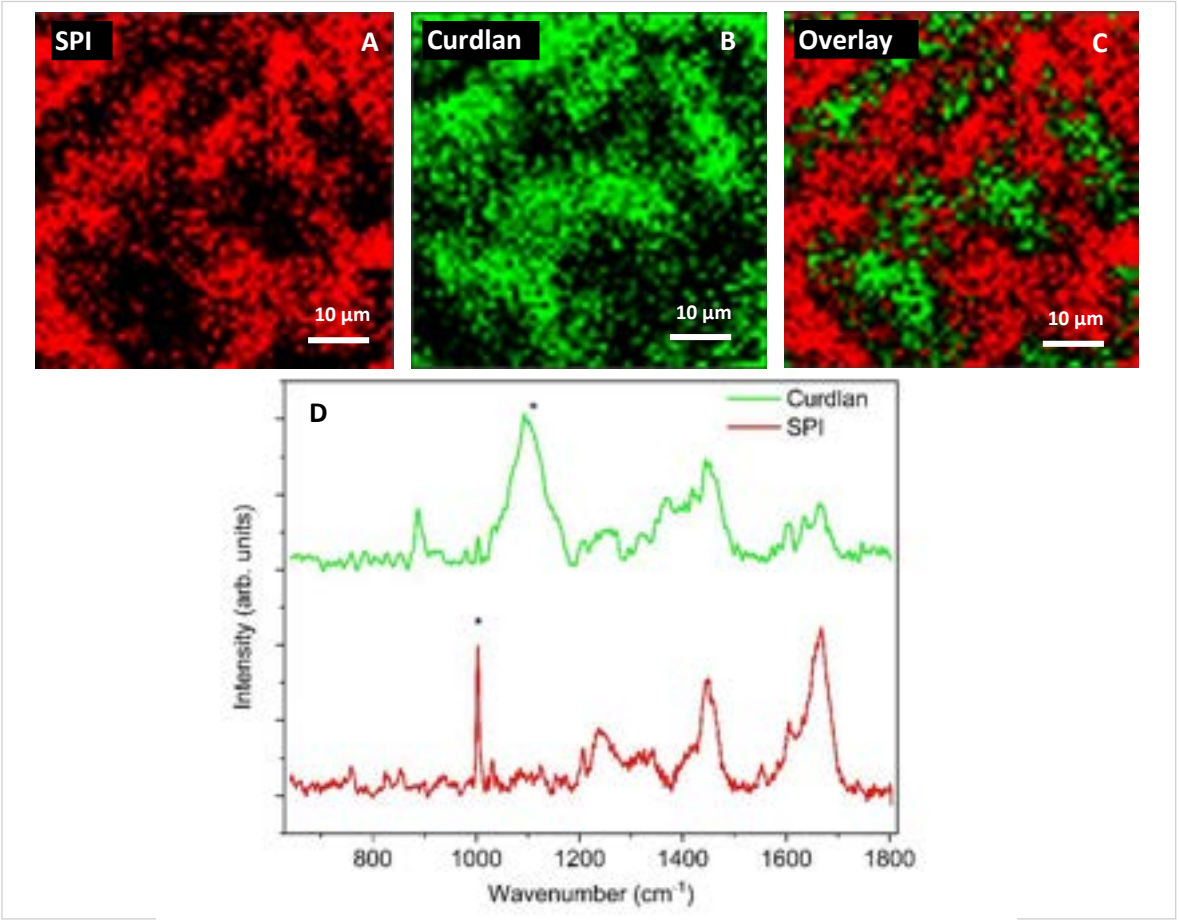

Figure 4. Results of Raman spectral imaging of prototypes comprising 18% (w/w) soy protein isolate (SPI) and 3% (w/w) curdlan. (A-C) Raman intensity maps showing the spatial distribution of (A) SPI, (B) curdlan, and (C) an overlay image of both components. Scale bar: 10µm. (D) Raman spectra of curdlan and SPI regions. Intensity of peaks marked with the asterisks was used to map the distribution of each component: 1130cm^{-1} for curdlan and 1000cm^{-1} for SPI.

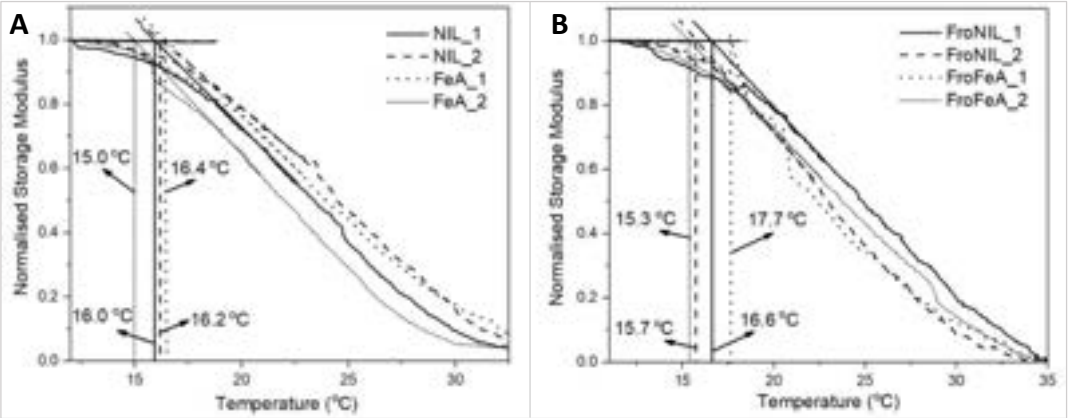

Figure 5. Duplicate graphs of dynamic mechanical analysis (in compression mode) for prototypes comprising 18% (w/w) soy protein isolate and 3% (w/w) curdlan, depicting the change in storage modulus following glass transition (onset temperatures indicated). The prototypes were pre-cut into cylindrical discs of 7.0-8.5 mm height and 13-14 mm diameter and analysed (A) after 1 day of storage at 4 °C, and (B) after 1 additional day of frozen (Fro) storage at -20 °C. The mixing stage of prototype preparation involved sequential addition of ingredients into 40-50 °C pH 6 solutions, namely (i) water [NIL, i.e., without phenolic acid nor trehalose] and (ii) ferulic acid (1.0 mM) + trehalose (2.0 mM) solution [FeA].

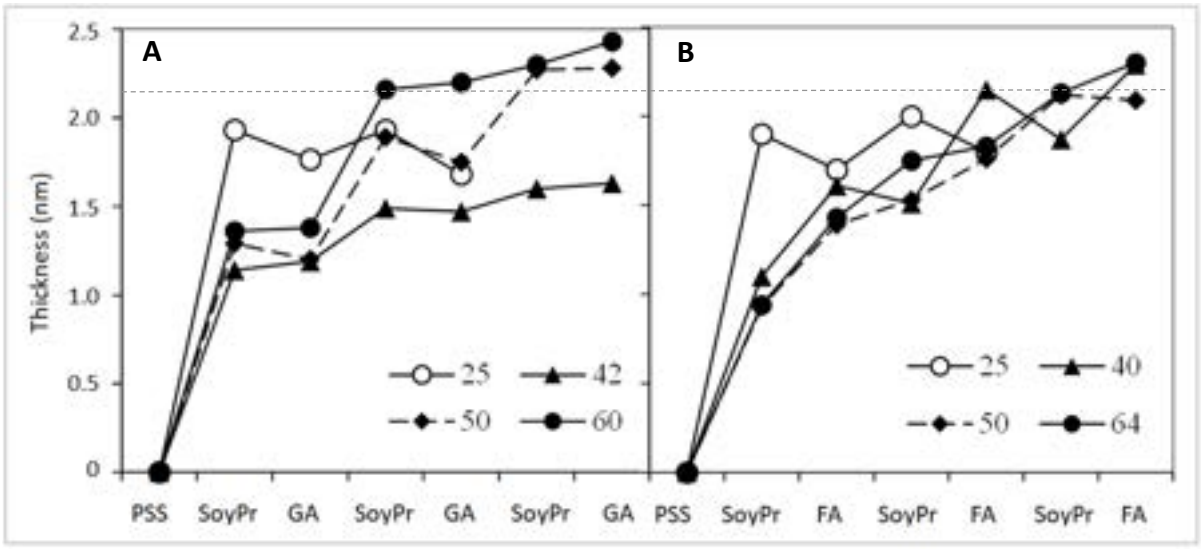

Figure 6. Precision ellipsometry measurement of increments in thickness of adsorbed layers atop poly-styrene-sulfonate (PSS) linker layer on silicon substrates. The order of adsorption was from left to right of the horizontal axis, namely: supernatant from defatted soy protein (SoyPr) isolate at pH 6, gallic acid (GA) in (A) and ferulic acid (FA) in (B). Different curves correspond to sample temperatures in degrees Celsius.

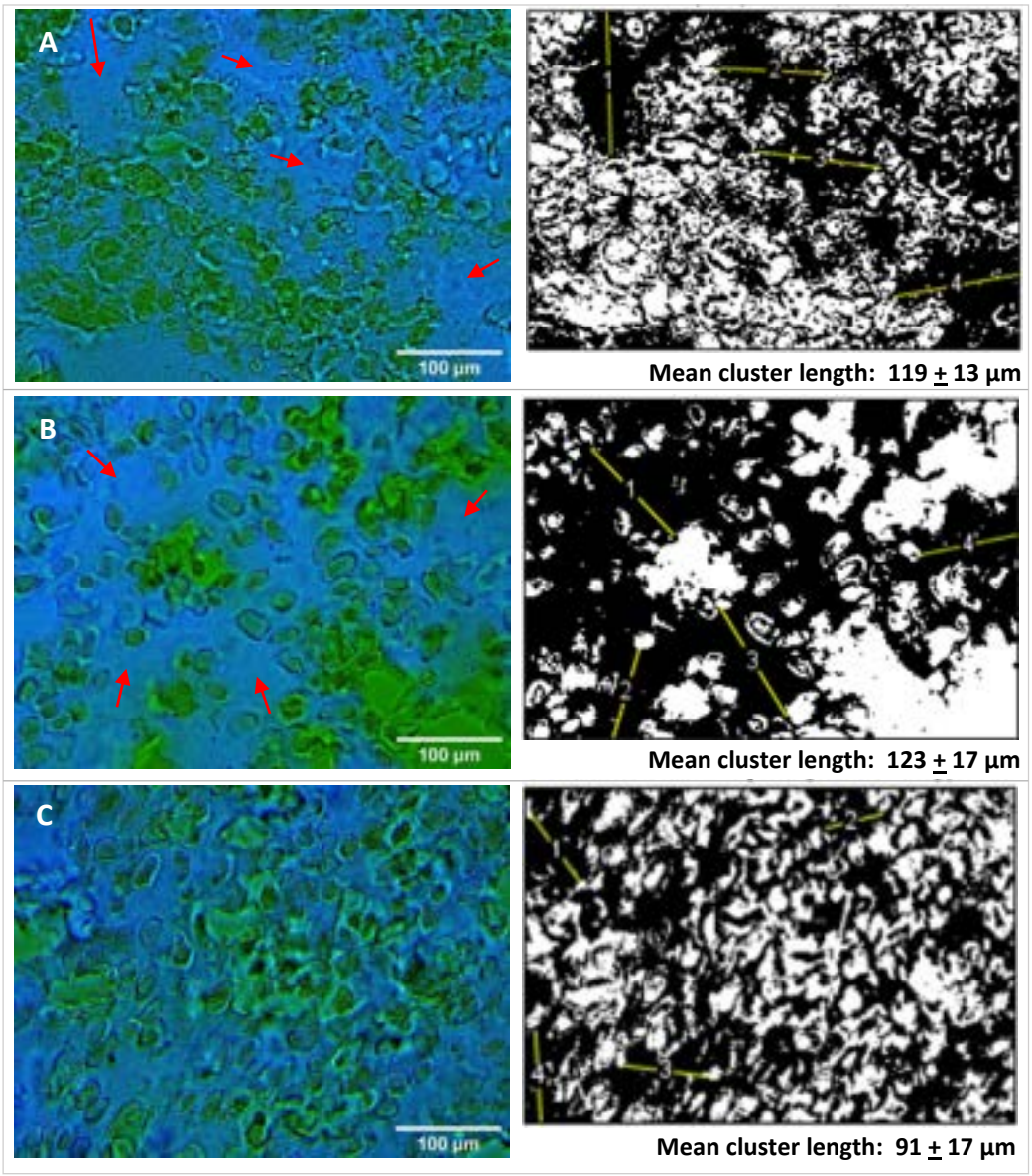

Figure 7. Epi-fluorescence micrographs (left) of prototypes comprising 18% (w/w) soy protein isolate (SPI) and 3% (w/w) curdlan, adjusted in brightness and contrast, and their corresponding binary images (right) showing the sizes of more discernible curdlan clusters. The mixing stage during prototype preparation involved sequential addition of ingredients into 40-50 °C pH 6 solutions, namely (A) water, (B) gallic acid (1.0 mM) solution, and (C) ferulic acid (1.0 mM) + trehalose (2.0 mM) solution. SPI was stained green by Fast Green FCR and curdlan was stained blue by sodium 8-anilino-1-naphthalenesulfonate. The red arrows indicate more expanded spatial zones of curdlan. Scale bar: 100 µm. Magnification: 20×.

Table 1. Change in stiffness of cooked fishball and various prototypes, from uniaxial compression stress-strain test at >70% strain at room temperature (RT). For analysis, the samples were pre-cut into cylindrical discs of 7.0-8.5 mm height and 13-14 mm diameter. (A) The effect of the type of phytochemical was tested. (B) Different concentrations of ferulic acid (most promising) were compared. (C) The impact of variation in process parameters was evaluated, specifically, (i) with preheating (*prh*) of ferulic acid at 65 °C for 1 h vs. without; (ii) mixing of ingredients with sequential addition vs. all at one go (*1-mix*); and (iii) mixing them at 40-50 °C vs. RT (*RT-mix*). The elastic modulus data at 60-70% strain was analysed by one-way ANOVA with Tukey HSD post-hoc test (n = 4). GAE: gallic acid equivalent; NIL: without phenolic acid nor trehalose; s.d.: standard deviation.

Samples	**Average change in stiffness and s.d. (kPa) at various ranges of % strain**						
	40-50%	s.d.	50-60%	s.d.	60-70%	s.d.	
(A)							*p ≤0.15*
Commercial fishball (BoBo brand)	214	24	532	84	**1,525**	305	***a***
Homemade fishball	252	9	434	21	935	92	*c*
Negative control: NIL	295	31	572	90	1,151	213	*bc*
Positive control: + Trehalose (2 mM)	247	8	457	32	897	113	*c*
Sample: Gallic acid (1.0 mM)	269	22	524	38	1,172	63	*bc*
Sample: Gallic acid (1.0 mM), *prh*	321	16	594	41	1,085	221	*bc*
Sample: Gallic acid (1.0 mM) + Trehalose (2.0 mM), *prh*	211	16	387	40	866	139	*c*
Sample: Ferulic acid (1.0 mM) + Trehalose (2.0 mM), *prh*	296	16	601	32	**1,416**	109	***ab***
Sample: Rice bran extract (1.0 mM GAE) + Trehalose (2.0 mM)	260	9	491	36	1,016	135	*c*
(B)							*p ≤0.15*
Negative control: NIL	295	31	572	90	1,151	213	*bc*
Sample: Ferulic acid (0.2 mM) + Trehalose (0.4 mM), *prh*	310	21	583	50	1,094	216	*c*
Sample: Ferulic acid (0.5 mM) + Trehalose (1.0 mM), *prh*	290	9	602	26	1,352	49	*ab*
Sample: Ferulic acid (1.0 mM) + Trehalose (2.0 mM), *prh*	296	16	601	32	**1,416**	109	***a***
Sample: Ferulic acid (2.0 mM) + Trehalose (4.0 mM), *prh*	280	9	562	21	1,306	61	*abc*
(C)							*p ≤0.10*
Negative control: NIL	295	31	572	90	1,151	213	*bcd*
Sample: Ferulic acid (1.0 mM) + Trehalose (2.0 mM), *prh, 1-mix*	257	13	489	26	1,068	52	*d*
Sample: Ferulic acid (1.0 mM) + Trehalose (2.0 mM), *prh, 1-mix, RT-mix*	239	16	484	51	1,122	149	*cd*
Sample: Ferulic acid (1.0 mM)	281	14	547	26	1,261	44	*abcd*
Sample: Ferulic acid (1.0 mM), *prh*	301	12	604	44	1,350	82	*abc*
Sample: Ferulic acid (1.0 mM) + Trehalose (2.0 mM), *prh, RT-mix*	271	17	562	38	1,380	88	*ab*
Sample: Ferulic acid (1.0 mM) + Trehalose (2.0 mM), *prh*	296	16	601	32	**1,416**	109	***a***
Sample: Ferulic acid (1.0 mM) + Trehalose (2.0 mM)	307	18	617	38	**1,420**	105	***a***

Table 2. Particle size measurements (± standard deviation) of 0.4% (w/w) defatted soy protein isolate dispersed in various pH 6 solutions, taken 1 day after heating at 99 °C for 10 min. NIL: without phenolic acid nor trehalose. *prh:* preheating of solution at 65 °C for 1 h, before the dispersion of protein. The results were analysed by one-way ANOVA with Tukey HSD post-hoc test (n = 3).

0.4% (w/w) soy protein isolate dispersions	**Average particle sizes (µm)**					
	d [4,3]		d [0.5]		d [0.9]	
		p ≤ 0.10		*p ≤ 0.10*		*p ≤ 0.10*
Negative control: NIL	192 ± 19	*d*	186 ± 30	*bc*	428 ± 26	*ab*
Positive control: + Trehalose (2.0 mM)	89 ± 3	*f*	36 ± 1	*e*	254 ± 21	*d*
Sample: + Gallic acid (1.0 mM), *prh*	241 ± 2	*ab*	218 ± 2	*ab*	425 ± 4	*ab*
Sample: + Gallic acid (1.0 mM) + Trehalose (2.0 mM), *prh*	259 ± 1	*a*	230 ± 1	*a*	480 ± 3	*a*
Sample: + Ferulic acid (1.0 mM)	207 ± 34	*bcd*	190 ± 31	*abc*	362 ± 60	*bc*
Sample: + Ferulic acid (1.0 mM), *prh*	167 ± 23	*d*	149 ± 19	*cd*	**299** ± 43	*cd*
Sample: + Ferulic acid (1.0 mM) + Trehalose (2.0 mM), *prh*	**145** ± 5	*e*	**115** ± 2	*d*	**284** ± 11	*d*

Declaration of interests

☒ The authors declare that they have no known competing financial interests or personal relationships that could have appeared to influence the work reported in this paper.

☐The authors declare the following financial interests/personal relationships which may be considered as potential competing interests:

Credit author statement

Pui Yeu Phoon: Conceptualisation, Formal analysis, Funding acquisition, Investigation, Methodology, Validation, Visualization, Writing - original draft, Writing - review & editing. **Amanda Sng Xin Yi**: Formal analysis, Investigation, Methodology, Validation, Visualization, Writing - review & editing. **Nikolai Yakovlev**: Formal analysis, Investigation, Methodology, Validation, Visualization, Writing - review & editing. **Lim Su Hui**: Formal analysis, Investigation, Methodology, Validation, Visualization, Writing - review & editing. **Nge Choy Eng**: Formal analysis, Methodology, Validation, Writing - review & editing. **Gomathy Sandhya Subramanian**: Formal analysis, Investigation, Methodology, Validation, Visualization, Writing - review & editing. **Sergey Gorelik**: Methodology, Validation, Writing - review & editing. **Yoganathan Kanagasundaram**: Validation, Writing - review & editing. **Maxim Kiryukhin**: Validation, Writing - review & editing.